

# Development of correlated quasiparticle conductance peak as molecule-linked gold nanoparticle films transition from Mott-insulator to metal phases

Patrick Joanis, Monique Tie, and Al-Amin Dhirani\*

*Department of Chemistry, University of Toronto, Toronto, Ontario, Canada, M5S 3H6*

(Dated: September 26, 2018)

We have studied conductance ( $g$ ) of butanedithiol-linked gold nanoparticle films across a percolation insulator-to-metal transition. As the transition proceeds, electrons become itinerant (i.e. Coulomb charging and kinetic effects are both significant), and films exhibit a previously unobserved zero-bias conductance peak (ZBCP). The peak is much more pronounced and easily observed using electromigration-induced break junction (BJ) contacts rather than macroscopic 4-probe electrodes. We attribute this ZBCP to quantum correlations amongst electrons, in view of other temperature- ( $T$ -) and magnetic ( $B$ -) dependent measurements as well as predictions of the Hubbard model and dynamic mean field theory in this transition regime. Metallic film resistances ( $R$ 's) increase linearly with  $T$ , but with suggested scattering lengths that, anomalously, are shorter than inter-atomic distances. Similar so-called “bad-metallic” behaviour has been observed in several studies of correlated systems, and is still being understood. We find here that the anomalous  $R$  behaviours are associated with the ZBCP. This system can serve as a new test bed for studying correlated electrons and points to a nano building-block strategy for fashioning novel correlated materials.

PACS numbers: 71.30.+h, 05.60.Gg, 81.07.Pr

Transitions where charges become itinerant while Coulomb interactions remain strong appear in a number of exotic materials, such as vanadium oxides that exhibit huge resistivity changes across an insulator-to-metal transition, cuprates that exhibit high  $T_c$  superconductivity and manganites that exhibit colossal magnetoresistance [1]. They have been intensely studied, and are known to arise in materials with partially open  $d$  and  $f$  orbitals, whose confined nature leads to strong electronic repulsion. As such materials transition from Mott insulating to metallic states, electrons interact with each other strongly and, therefore, move in a correlated fashion. Calculations combining a local density approximation with dynamic mean field theory [1] predict that as the transition proceeds, the upper and lower Hubbard bands become more closely spaced, and a quasiparticle peak develops at the Fermi level. Experimentally, a quasiparticle peak has been observed in vanadium oxide via optical [2] and photoemission [3] spectroscopy and in  $\text{NiS}_{2-x}\text{Se}_x$  via tunneling spectroscopy [4].

Films of Au nanoparticles (NPs) cross-linked with  $n$ -alkanedithiol ( $\text{HS}(\text{CH}_2)_n\text{SH}$ , e.g. taking  $n = 4$ ) can exhibit a thickness-driven insulator-to-metal percolation transition in which both Coulomb and kinetic effects can be significant, suggesting that this system can potentially serve as a novel and potentially advantageous test bed for studying electron correlations [5–7]. Use of prefabricated NPs with relatively narrow size distribution limits averaging [8]. Further, except for a small fraction of NPs that self-assemble to the functionalized surface, nanoparticle films (NPFs) grow by NPs attaching to one another, forming metallic pathways in a fractal-like rather than 2-D manner. As a result, the percolation transition is gradual, and phases that are intermediate between insulating and metallic extremes are more easily observed.

In the present study we explore the evolution of conductance ( $g$ ) for butanedithiol-linked NPFs as a function of temperature ( $T$ ) and bias ( $V$ ) across the percolation insulator-to-metal transition. Previous studies of other systems have shown that as the transition proceeds, first, nanoscale metallic puddles with exotic quasiparticles form [2, 9]. In order to better observe these exotic phases, we use break junctions (BJs) to interrogate nanoscale electrical properties of the NPFs. We also studied macroscopic properties of films using four-probe electrodes. As the NPFs become metallic, both BJ and four-probe samples exhibit a zero-bias conductance peak (ZBCP) that we attribute to correlated quasiparticles. We find that scattering lengths, estimated assuming Boltzman transport, are smaller than inter-atomic separations, implying “bad metallic” behaviour that has been attributed to correlation effects in other systems but whose origin has been unresolved. As with other bad metals, NPF  $R$ 's increases linearly with  $T$ . We find here that this behaviour can be traced to the ZBCP.

Both four-probe and BJ samples were fabricated on glass substrates that were first cleaned by immersion in hot piranha for 30 min and then functionalized by immersion in a boiling toluene solution of 3-mercaptopropyltrimethoxysilane for 20 min. For BJ samples, a Au wire that was a  $100\ \mu\text{m}$  wide, 8 mm long, 16 nm thick in the middle (over a  $100\ \mu\text{m}$  stretch), and 150 nm thick over the rest of its length was deposited using metal evaporation and shadow masks. A ramped voltage was applied in  $\text{L-N}_2$  until the wire broke due to electromigration. BJs exhibited gaps with widths that ranged from a few  $\mu\text{m}$  to a few nm (estimated from measurements of tunnel currents). For four-probe samples, Au electrodes  $\sim 6$  mm long, 200 nm thick and separated by 2 mm were employed. For both types of samples, copper

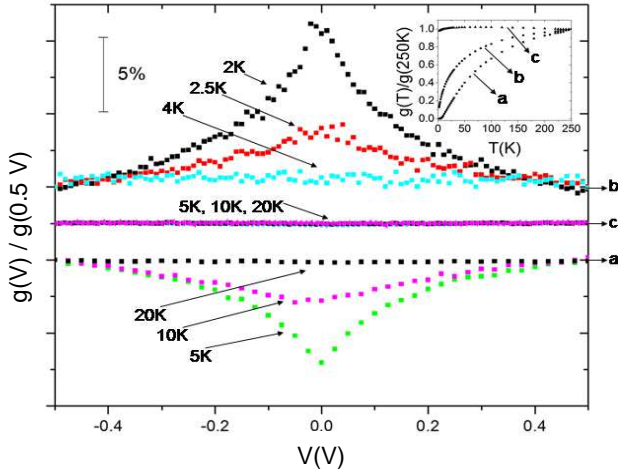


FIG. 1:  $g$  vs.  $V$  at different  $T$  (main panel) and  $g$  vs.  $T$  at  $V = 0$  (inset) obtained using a four-probe electrode configuration. All the data were obtained using the same sample at different film thicknesses. Data in the main panel and inset with the same labels correspond to the same sample thickness, namely 12-, 18- and 25- one-hour exposures to Au NP solution, labeled “a” to “c”, respectively, in order of increasing thickness. The data in the main panel for a given thickness and  $T$  have been normalized to their respective values at 0.5 V and offset for clarity.

magnet wires were soldered to the Au electrodes using indium before film self-assembly. Au NPs  $5.0 \pm 0.8$  nm in diameter were synthesized using published methods [6], and butanedithiol used to link Au NPs was purchased and used as received. NPFs were self-assembled by alternately immersing the slides in an Au NP solution for 10-60 min and a 0.5 mM ethanolic butanedithiol solution 10 min until a desired  $R$  was reached.  $g$  at various  $V$ 's were determined using lockins and at various  $T$ 's using a Quantum Design PPMS. To confirm reproducibility, the evolution of four BJ and a pair of four-probe samples were studied in detail, each at several NPF thicknesses.

Figure 1 plots  $g$  vs.  $T$  and  $V$  for a four-probe sample. The data were obtained using the same sample at three different NP/dithiol exposure cycles corresponding to behaviour that is insulating, just metallic and well metallic - graphs labeled “a”, “b” and “c”, respectively. In the insulating regime,  $g \rightarrow 0$  as  $T \rightarrow 0$  and, concurrently,  $g$  is suppressed near zero volts. This suppression is observed in both two- and four-probe measurements performed simultaneously on the same sample, indicating that at this thickness, film  $R$  dominates over contact  $R$ . When thickness increases so the sample is just at the transition, remarkably the four-probe data exhibit a ZBCP at low  $T$ . The two-probe data continue to show a small suppression of  $g$  as before (data not shown). These data indicate that the ZBCP observed in the four-probe data is a film effect and that the suppression observed in the two-probe data arises from a small barrier at the contact(s). As  $T$  in-

creases (beyond 2K to 10K depending on the sample), the ZBCP wanes and  $g$  becomes independent of  $V$  (ohmic). As film thickness increases still further, four-probe  $g$  data behave essentially ohmically even at the lowest accessible  $T$ . Simultaneously measured two-probe  $g$  data continue to exhibit the presence of a small barrier.

Insulating film behaviour is consistent with single electron charging phenomena (Coulomb blockade) [10]. Below a percolation threshold, electrons tunnel on to and must charge NPs or metallic clusters of NPs. Previous studies have shown that single-electron charging energies increase with decreasing particle size and can become substantial at nm length scales [10]; e.g. the single electron charging energy of a 1 nm sphere can be estimated using Coulomb's law as  $\sim 1$  eV. This Coulomb barrier leads to suppression of  $g$  at low  $V$  and  $T$  in NPFs.

A variety of processes are known to cause ZBCPs. Reflectionless tunneling can be excluded here because it is a contact rather than a film phenomenon, while ZBCP appear in measurements of film  $g$ . Lack of Zeeman splitting excludes the Kondo effect. The field ( $B$ ) at which Zeeman peak splitting would be expected for a zero-bias anomaly (Kondo effect) can be estimated using the Haldane relation:  $2\mu_B B \sim k_B T_K = \sqrt{\Gamma U}/2 \cdot \exp[-\pi\epsilon_0(-\epsilon_0 + U)/\Gamma U]$  where  $\mu_B$  is the Bohr magneton,  $\epsilon_0$  is the energy level through with transport occurs,  $U$  is the on-site repulsion, and  $\Gamma$  is the energy broadening [11, 12]. Since there are no magnetic impurities in our system (otherwise a Kondo peak would be observed even in thick films), we attribute any potential Kondo effect to a mechanism based on single electron charging. An Arrhenius plot of  $g$  vs.  $T$  for a non-metallic film (Fig. 2a, inset) yields a temperature scale of 30 K. Using this as an estimate for  $\epsilon_0$ ,  $U \sim 2\epsilon_0$ , and  $\Gamma \sim \epsilon_0$ , splitting should then be observed for  $B \sim 3T$ . We applied  $\sim 3$ -5 times this field, but did not observe peak splitting, even with  $< 1\%$  sensitivity to changes in  $g$ . Joule heating can also be excluded because  $g$  increases with  $T$  (Fig. 1, inset). Heating caused by increasing  $V$  should cause  $g$  to increase and should generate a zero-bias conductance suppression, rather than a peak as observed.

Using BJs to measure  $g$  improves resolution of spectroscopic features and reveals a mesoscale origin of the ZBCP. Figure 2 shows nanoscale film behaviour as the insulator-to-metal transition progresses.  $g$  vs.  $V$  data for an insulating NPF (Fig. 2a, main panel) show strong Coulomb blockade suppression near 0 V at 2 K, and zero-bias  $g$  vs.  $T$  data (inset) show that  $g \rightarrow 0$  as  $T \rightarrow 0$ . As the film was subjected to more NP/dithiol immersion cycles, it eventually became metallic ( $g \rightarrow$  non-zero constant as  $T \rightarrow 0$ ) but with a persistent small energy barrier since  $g$  was observed to increase with both  $V$  and  $T$  (data not shown). When  $V$  was increased to a few volts at low  $T$ ,  $g$  suddenly and irreversibly increased 10- to 100-fold remaining stable thereafter, and the (contact) barrier was no longer observed. All BJ samples with suffi-

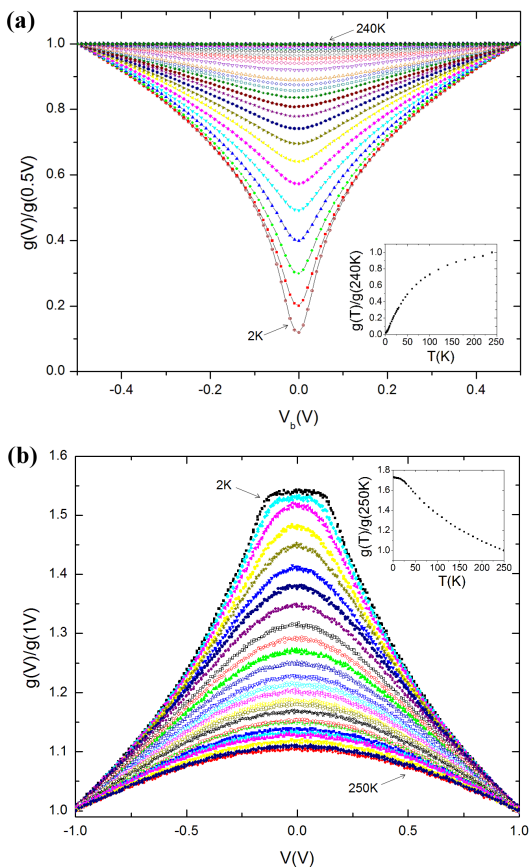


FIG. 2: Evolution of  $g$  measured using a BJ as a NPF crosses the insulator-to-metal transition. a.  $g$  vs.  $V$  at different  $T$ 's from 2 K to 240 K (main panel) and  $g$  vs.  $T$  at  $V = 0$  (inset) for an insulating, 10 dithiol/NPF. Data for a given  $T$  have been normalized to their respective values at 0.5 V. The conductance at 250 K is  $9.39 \times 10^{-5} \Omega^{-1}$ . Data were obtained at 2K to 30K in 1K steps, 30K to 50K in 5K steps, 50K to 100K in 10K steps and 100K to 240K in 20K steps. b.  $g$  vs.  $V$  at different  $T$ 's from 2 K to 250 K (main panel) and  $g$  vs.  $T$  at  $V = 0$  (inset) for the same sample as in a. with a thicker (50 dithiol/nanoparticle exposure) film that has turned metallic. Data for a given temperature have been normalized to their respective values at 0.5 V. The conductance at 250 K is  $0.02 \Omega^{-1}$ . Data were obtained at 2K to 30K in 1K steps, 30K to 50K in 5K steps, and 50K to 250K in 10K steps.

ciently thick NPF bridges exhibited this break down after which pronounced ZBCPs became apparent. The peaks exhibit an Ohmic plateau region at low  $V$  (Fig. 2b, main panel) and survive to high  $T$ 's - at least 250 K, beyond which the data tend to become noisy. The significantly larger energy scale provided by the voltage ( $\sim$  eV) arises from peak broadening due to voltage division across the film. As more dithiol/NP is self-assembled, eventually  $g$ 's and peak widths change only slightly, suggesting that most of the current flows through a portion of the NPF located in the gap between Au electrodes. We attribute the ZBCPs to the formation of a “meso-metallic” phase since 1) they are associated with non-zero  $g$  at low  $T$

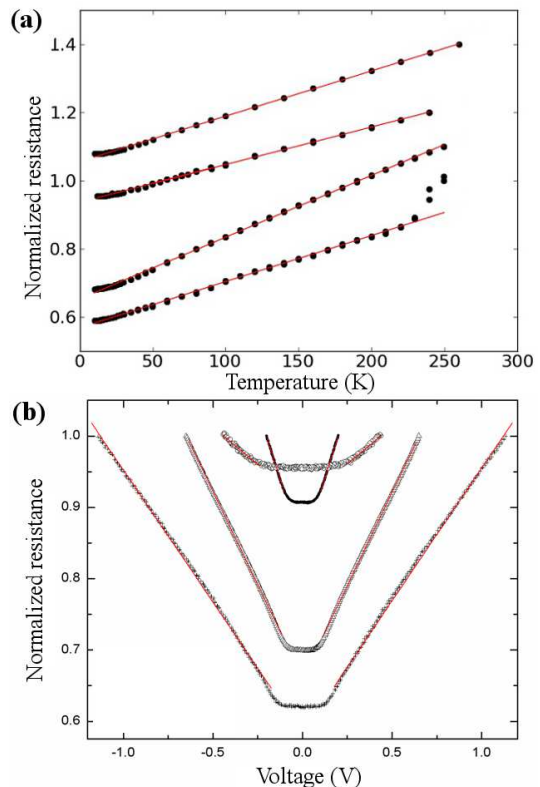


FIG. 3:  $R$  vs.  $T$  and vs.  $V$  data for metallic NPFs measured using BJ. a.  $R$  vs.  $T$  at  $V = 0$  for four metallic NPFs. b.  $R$  vs.  $V$  at 4 K for the same four samples as in a. Data are fit to straight lines over a portion of their respective ranges as shown. All data have been normalized using their respective maximum values and offset in a. for clarity.

(i.e. films are metallic - see Fig. 2b, inset); 2)  $g$  is not entirely ohmic (the peaks have an ohmic plateau below a threshold  $V$  but decreasing  $g$  above); and 3) the ZBCPs are more pronounced in BJ samples than in macroscopic four-probe samples. This attribution is also consistent with dynamic mean field calculations using the Hubbard model that predict the development of a peak in the density of states at the Fermi level at the onset of metallicity.

Metallic states of various correlated materials - such as organic conductors, alkali-doped C60 as well as those of various oxides (including cuprates, manganites and vanadium dioxide) - exhibit a linear increase of  $R$  with  $T$  and quasiparticle scattering lengths that, remarkably, are smaller than interatomic distances. Similar behaviours are observed here (see below). Such “bad metallic” behaviours are still being elucidated in the literature [2, 13]. It is generally agreed, however, that the quasiparticle picture of a particle with a well defined momentum on the order of the Fermi momentum experiencing occasional scattering breaks down in these systems as a result of strong electron-electron correlations. Figures 3a and 3b plot zero-bias  $R$  vs.  $T$  and  $R$  vs.  $V$  data for four BJ samples. The data indicate that  $T$  independent scatter-

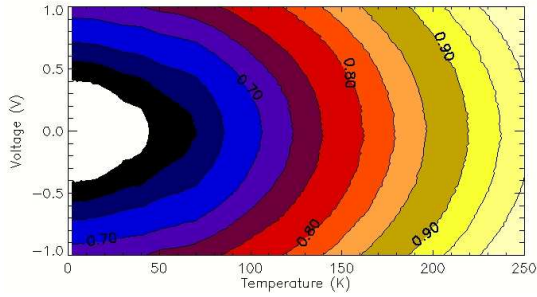


FIG. 4: A contour plot of  $R$  at various  $V$ s and  $T$ s using the same data shown in Fig. 3. The data have been normalized to their maximum  $R$ , and contour labels denote fractions of this maximum.

ing dominates  $R$  in these NPFs. Given the nanogranular nature of NPFs, ubiquitous  $T$  independent elastic scattering from NP interfaces might be expected. However, assuming uncorrelated electrons that scatter occasionally (Boltzman transport) for arguments sake, the resistivity would be given by  $\rho = 3\pi^2\hbar/e^2k_F^2l$ , where  $\rho$  is the resistivity,  $\hbar$  is Planck's constant,  $e$  is the quantum of charge,  $k_F$  is the Fermi wave vector and  $l$  is the scattering length [14]. For our BJ samples, taking a typical  $R$  of  $\sim 50 \Omega$ , a sample area of  $150 \mu\text{m} \times 100 \text{nm}$ , a sample length of  $100 \text{nm}$ , and assuming a Fermi wavelength of  $0.54 \text{nm}$  for gold, we estimate  $l \sim 10^{-3} \text{\AA}$ . For our four-probe samples, taking a typical  $R$  of  $\sim 200 \Omega$ , a sample area of  $3 \text{mm} \times 100 \text{nm}$ , a sample length of  $3 \text{mm}$ , and assuming a Fermi wavelength of  $0.54 \text{nm}$ , we estimate  $l \sim 0.3 \text{\AA}$ . These are rough estimates because of uncertainties in film thickness, but it is safe to conclude that the predicted scattering lengths in the nanoscale BJ samples are smaller than interatomic distances and smaller than those for the macroscopic samples. This increased tendency for bad metallic behaviour at smaller length scales is correlated with the ZBCP being more pronounced in the BJ samples. This is also consistent with scan probe studies by others that have shown that correlated materials are heterogeneous [2, 9, 15]. As the insulator-to-metal transition proceeds, nanoscale metallic puddles form and grow; these regions are not smaller versions of fully formed bulk metallic state.

Correlated systems, e.g. the cuprates, in addition to exhibiting anomalously large resistance, exhibit  $R$  that increases linearly with  $T$  to very high  $T$ . This behaviour is not well understood [13]. Figures 3a and b show that both  $R$  vs.  $T$  at zero-bias and  $R$  vs.  $V$  at low  $T$  are constant initially and then both vary linearly for all four BJ samples. Figure 4 plots contour lines for  $R$  vs.  $V$  and  $T$  data for one of the samples. Equally spaced contour lines reflect the underlying linearity of  $R$  as a function of either variable. That is, this study suggests that both behaviours can be traced back to the quasiparticle peak in the density of states. Further theoretical work

modeling transport measurements and exploring this link would be beneficial. Another significant implication of the present study is that it suggests that nanostructured materials constitute a novel class of correlated materials since Coulomb interactions in nanostructures are inherently large and, as electrons become itinerant, both Coulomb and kinetic effects should be significant. Such materials can provide a new, controllable and potentially rich platform to study these exotic phenomena since there is a tremendously wide and, indeed, designable selection of nanostructures that can be used as material building blocks.

We thank Y.-B. Kim for discussions. This work was supported by the Natural Science and Engineering Research Council for Canada.

---

\* Electronic address: adhirani@chem.utoronto.ca

- [1] G. Kotliar and D. Vollhardt, *Physics Today* March, 53 (2004). G. Kotliar et al., *Rev. Mod. Phys.* **78**, 865 (2006). K. Held, *Adv. Phys.* **56**, 829 (2007). M. Jarrell, *Phys. Rev. Lett.* **69**, 168 (1992).
- [2] M. M. Qazilbash et al., *Science* **318**, 1750 (2007).
- [3] S.-K. Mo et al., *Phys. Rev. Lett.* **90**, 186403 (2003).
- [4] K. Iwaya et al., *Phys. Rev. B* **70**, 161103R (2004).
- [5] M. Brust et. al, *Adv. Mater.* **7**, 795 (1995). A. Zabet-Khosousi, P. E. Trudeau, Y. Suganuma, A.-A. Dhirani and B. Statt, *Phys. Rev. Lett.* **96**, 156403 (2006).
- [6] N. Fishelson et al, *Langmuir* **17**, 403 (2001).
- [7] M. Brust and C. J. Kiely, *Colloids Surf. A* **202**, 175 (2002). A. Zabet-Khosousi and A.-A. Dhirani, *Chem. Rev.* **108**, 4072 (2008).
- [8] K. C. Beverly, J. F. Sampaio and J. R. Heath, *J. Phys. Chem. B* **106**, 2131 (2002).
- [9] E. Dagotto, *Science* **309**, 257 (2005). M. Uehara et al., *Nature* **399**, 560 (1999).
- [10] S. Chen et al., *Science* **280**, 2098 (1998). A. W. Snow and H. Wöhlthjen, *Chemistry of Materials* **10**, 947 (1998). B. Abeles et al., *Adv. Phys.* **24**, 407 (1975). P. E. Trudeau, A. Escorcica and A.-A. Dhirani, *J. Chem. Phys.* **119**, 5267 (2003).
- [11] L. I. Glazman and M. E. Raikh, *JETP Lett.* **47**, 452 (1988). J. Park et al., *Nature* **417**, 722 (2002). W. Liang et al., *Nature* **417**, 725 (2002).
- [12] F. D. M. Haldane, *Phys. Rev. Lett.* **40**, 416 (1978).
- [13] P. B. Allen, R. M. Wentzcovitch, W. W. Schulz and P. C. Canfield, *Phys. Rev. B* **48**, 4359 (1993). M. Qazilbash et al., *Phys. Rev. B* **74**, 205118 (2006). V. J. Emery and S. A. Kivelson, *Phys. Rev. Lett.* **74**, 3253 (1995). V. J. Emery, S. A. Kivelson and J. M. Tranquada, *Proc. Natl. Acad. Sci.* **96**, 8814 (1999). O. Gunnarsson and J. E. Han, *Nature* **405**, 1027 (2000).
- [14] O. Gunnarsson, M. Calandra, and J. E. Han, *Rev. Mod. Phys.* **75**, 1085 (2003).
- [15] K. K. Gomes et al., *Nature* **447**, 569 (2007). L. Jinho et al., *Nature* **442**, 546 (2006). K. M. Lang et al., *Nature* **415**, 412 (2002). S. H. Pan et al., *Nature* **413**, 282 (2001).